

Article

Toxicity Evaluation and Controlled-Release of Curcumin-Loaded Amphiphilic Poly-N-vinylpyrrolidone Nanoparticles: In Vitro and In Vivo Models

Anna L. Luss ^{1,*} , Dmitry V. Bagrov ² , Anne V. Yagolovich ² , Ekaterina V. Kukovyakina ¹, Irina I. Khan ^{3,4} , Vadim S. Pokrovsky ^{3,4} , Maria V. Shestovskaya ¹ , Marine E. Gasparian ^{1,5} , Dmitry A. Dolgikh ^{2,5}  and Andrey N. Kuskov ¹ 

¹ Department of Technology of Chemical, Pharmaceutical and Cosmetic Substances, D. Mendeleev University of Chemical Technology of Russia, 125047 Moscow, Russia; kev0700@yandex.ru (E.V.K.); marieshestovskaya@gmail.com (M.V.S.); marine_gasparian@yahoo.com (M.E.G.); kuskov.a.n@muctr.ru (A.N.K.)

² Faculty of Biology, Lomonosov Moscow State University, 119234 Moscow, Russia; bagrov@mail.bio.msu.ru (D.V.B.); anneyagolovich@gmail.com (A.V.Y.); dolgikh@nmr.ru (D.A.D.)

³ N.N. Blokhin National Medical Research Center of Oncology, Ministry of Health of Russia, 115478 Moscow, Russia; vadimpokrovsky@yandex.ru (V.S.P.)

⁴ Department of Biochemistry, People's Friendship University of Russia (RUDN University), 117198 Moscow, Russia

⁵ Shemyakin-Ovchinnikov Institute of Bioorganic Chemistry of the Russian Academy of Sciences, 117997 Moscow, Russia

* Correspondence: al.luss@yandex.ru

Abstract: Curcumin attracts huge attention because of its biological properties: it is antiproliferative, antioxidant, anti-inflammatory, immunomodulatory and so on. However, its usage has been limited by poor water solubility and low bioavailability. Herein, to solve these problems, we developed curcumin-loaded nanoparticles based on end-capped amphiphilic poly(N-vinylpyrrolidone). Nanoparticles were obtained using the solvent evaporation method and were characterized by dynamic and electrophoretic light scattering, transmission electron (TEM) and atomic force (AFM) microscopy. The average particle size was 200 nm, and the ζ -potential was -4 mV. Curcumin-release studies showed that nanoparticles are stable in aqueous solutions. An in vitro release study showed prolonged action in gastric, intestinal and colonic fluids, consistently, and in PBS. In vitro studies on epidermoid carcinoma and human embryonic kidney cells showed that the cells absorbed more curcumin in nanoparticles compared to free curcumin. Nanoparticles are safe for healthy cells and show high cytotoxicity for glioblastoma cells in cytotoxicity studies in vitro. The median lethal dose was determined in an acute toxicity assay on zebrafish and was 23 μ M. Overall, the curcumin-loaded nanoparticles seem promising for cancer treatment.

Keywords: curcumin; poly(N-vinylpyrrolidone); nanoparticles; glioblastoma; toxicity



Citation: Luss, A.L.; Bagrov, D.V.; Yagolovich, A.V.; Kukovyakina, E.V.; Khan, I.I.; Pokrovsky, V.S.; Shestovskaya, M.V.; Gasparian, M.E.; Dolgikh, D.A.; Kuskov, A.N. Toxicity Evaluation and Controlled-Release of Curcumin-Loaded Amphiphilic Poly-N-vinylpyrrolidone Nanoparticles: In Vitro and In Vivo Models. *Pharmaceutics* **2024**, *16*, 8. <https://doi.org/10.3390/pharmaceutics16010008>

Academic Editor: Gabriele Grassi

Received: 20 November 2023

Revised: 13 December 2023

Accepted: 16 December 2023

Published: 19 December 2023



Copyright: © 2023 by the authors. Licensee MDPI, Basel, Switzerland. This article is an open access article distributed under the terms and conditions of the Creative Commons Attribution (CC BY) license (<https://creativecommons.org/licenses/by/4.0/>).

1. Introduction

In recent years, micelles have been studied as one of the most promising strategies for site-specific drug delivery. One of the most well-known polymers for creating micellar delivery systems is polyethylene glycol (PEG) [1–3]. Despite the well-studied chemistry of PEG, there is currently an active search for alternative polymers/copolymers for the delivery of physiologically active substances with similar properties. Polylactide [4,5], poly(lactide-co-glycolide) [6–8], poly(ϵ -caprolactone) [9,10] and others are also used as carriers.

In the last decade, interest has arisen in carriers based on poly(N-vinylpyrrolidone) (PVP) [11,12]. Like PEG, PVP has a very long history of medical use [13,14]. From a pharmaceutical point of view, it has attracted significant interest due to certain physicochemical

properties: solubility in almost all solvents, affinity for hydrophobic and hydrophilic surfaces, ability to form complexes, superior bioavailability and biocompatibility [13]. PVP is widely used in medicine as an antiseptic in combination with iodine and as a component of solutions for contact lenses [15,16]. Moreover, it is included in the FDA's database of inactive ingredients for use in oral, topical and injectable pharmaceutical products [17].

Amphiphilic PVP derivatives with hydrophobic terminal groups have been studied over the past decades as intravenous drug delivery systems [18–20]. They self-organize in aqueous solutions to form micellar structures and demonstrate excellent hemo- and biocompatibility. Compared to standard nanoparticles (PLGA, PLA, etc.), such aggregates have a hydrophilic outer shell and inner hydrophobic core, which allows the encapsulation of hydrophobic substances with high efficiency without any stabilizers. Parameters such as the copolymer molecular weight, morphology and size of the micelles are easily controlled during the synthesis process. They can capture various therapeutic agents, such as non-steroidal anti-inflammatory drugs [19–21], antitumor drugs [22], antifungal antibiotics [23], cytokines [24,25] and plasmid DNA [26] in micelles. Depending on the average hydrodynamic radius, nanoparticles can be absorbed by cell cultures through various mechanisms, including endocytosis and membrane fusion, which allows selective delivery of the active substance to both the cell's endosomes and its nucleus [27]. In addition, PVP nanoparticles can be used as effective modifiers of liposomal membranes, increasing their stability [23].

Curcumin is a natural polyphenol found in turmeric. Its clinical potential is determined by anti-inflammatory [28], antimicrobial [29], anticarcinogenic [30,31], hypoglycemic [32,33] and immunomodulating [34] and other properties. Curcumin has a very promising property, namely increased uptake by tumor cells *in vitro*. Moreover, its pro-apoptotic effect increases with increasing intracellular concentration, which may be promising in the development of drugs against malignant neoplasms, including glioblastoma and colorectal cancer [35–39]. Curcumin has also been shown to be effective not only as an anticancer drug but also in the fields of oral hygiene, periodontal therapy, gastrointestinal diseases, ophthalmic drugs and wound healing [37]. Despite its wide range of biological activities, curcumin has low bioavailability due to its poor solubility in aqueous media and low stability in the presence of air and UV radiation [40,41]. These limitations represent a major problem to the study and application of curcumin in biomedicine. A solution to this problem could be the effective encapsulation of curcumin into nanoparticles [42].

Herein, we report the preparation of curcumin-loaded nanoparticles based on amphiphilic PVP end-capped with a tioctadecyl group. PVP with a molecular weight of 6 kDa was selected based on previous studies as the most suitable candidate to achieve maximum encapsulation of curcumin by its lipophilic–lyophobic balance. Nanoparticles were prepared by the solvent evaporation method. The anticancer activity of curcumin-loaded PVP was estimated in glioblastoma cell lines. In addition, *in vitro* release dynamics were measured in various environments, and the acute toxicity of zebrafish *in vivo* was noted.

2. Materials and Methods

2.1. Materials

N-vinylpyrrolidone and octadecyl mercaptan (ODM) were obtained from Sigma-Aldrich (St. Louis, MO, USA). Azobisisobutyronitrile (AIBN) was obtained from Chemical Line (St. Petersburg, Russia). 1,4-dioxane was obtained from LenReaktiv (St. Petersburg, Russia). Curcumin was obtained from MT BIO-TECH (Changsha, China). All chemicals were used without further purification unless otherwise stated. Phosphate-saline buffer (PBS) were obtained from Servicebio (Wuhan, China). All solvents and components of buffer solutions were used as received.

2.2. Synthesis and Physicochemical Characteristics of Nanoparticles Based on Amphiphilic Poly(N-vinylpyrrolidone)

2.2.1. Synthesis of Amphiphilic Poly(N-vinylpyrrolidone)

The synthesis of amphiphilic poly(N-vinylpyrrolidone) with a molecular weight of 6 kDa was carried out in accordance with [18,27,43]. Briefly, 20 mL of N-vinylpyrrolidone, AIBN 1 wt% (0.7 mol%) and ODM 0,25 wt% (1 mol%) were dissolved in 40 mL of 1,4-dioxane. The reaction was carried out at 70°C for 3 h. The resulting solution was dialyzed against water, frozen and freeze-dried. Molecular weight was determined by reverse iodometric titration according to the method described by the authors in [44] and it was 6 kDa. The absence of solvent residues was determined by thermogravimetric analysis.

2.2.2. Synthesis of Curcumin-Loaded Nanoparticles Based on Amphiphilic Poly(N-vinylpyrrolidone)

A 90 mg sample of amphiphilic poly(N-vinylpyrrolidone) was dissolved in 30 mL of water (3 mg/mL), and 4 mL of curcumin solution in acetone (2.5 mg/mL) was added to the resulting solution. Then the resulting mixture was dispersed on an ultrasonic homogenizer Bandelin SONOPULS HD 4400 (Berlin, Germany) in the 1-s-on/1-s-off mode with an amplitude of 25% for 20 min. Then, the solvent was distilled off using a Heidolph Hei-VAP Ultimate rotary evaporator (Schwabach, Germany), and the resulting suspension of nanoparticles (PVP-Cur NPs) was centrifuged at 4000 rpm. Supernatant was frozen and freeze-dried.

2.2.3. Determination of Particle Size and Surface Charge

The ζ -potential and hydrodynamic diameter of the nanoparticles were determined by dynamic light scattering (DLS) and electrophoretic light scattering (ELS) using a Malvern Zetasizer Nano Z&S (Worcestershire, UK). Measurements were carried out at 25 °C and in distilled water three times for each sample.

2.2.4. Transmission Electron Microscopy and Atomic Force Microscopy

The PVP-Cur NPs were visualized using transmission electron microscopy (TEM) and atomic force microscopy (AFM). For both imaging procedures, the NPs were deposited onto carbon-formvar TEM grids (mesh 200, Electron Microscopy Science, Hatfield, PA, USA). The grids were treated using a glow discharge device K100X (Emitech, currently Quorum Technologies, Laughton, UK) at 30 mA for 30 s. For the TEM imaging, the sample was diluted in water to $c = 0.1$ mg/mL, deposited onto the grids for approximately 1 min and then the grids were stained by 1% uranyl acetate and dried. Images were carried out using a JEM-1400 electron microscope (JEOL, Tokyo, Japan) operating at 120 kV, equipped with Rio-9 camera (Gatan Inc., Pleasanton, CA, USA).

For the AFM imaging, the sample was diluted in water to $c = 0.25$ mg/mL, deposited onto the grids for approximately 1 min and then the grids were washed with water and dried. The images were acquired in semicontact mode, using a Solver PRO-M microscope (NT-MDT, Zelenograd, Russia). The scanning rate was 1–1.7 Hz, and the NSG10 cantilevers (Tips-Nano, Moscow, Russia) were used (typical curvature radius 6 nm, typical force constant $k = 11.8$ N/m).

Image processing was carried out using Fiji [45] and FemtoScan Online [46] for the TEM images and AFM frames, respectively.

2.2.5. Evaluation of Curcumin Encapsulation in the PVP-Cur NPs

The curcumin encapsulation efficiency was calculated by ratio of total curcumin content in PVP-Cur NPs to total drug amount according to [47]. The percent of loaded drug was calculated from the total amount of drug extracted from the PVP-Cur NPs to the known weight of the nanoparticles. To extract curcumin, lyophilized PVP-Cur NPs were dissolved in acetonitrile (5 mg in 5 mL). The samples were stirred at 500 rpm for 2 h for full curcumin extraction. Then the samples were centrifuged at 10,000 rpm and supernatants were col-

lected. Suspension (20 µL) was dissolved in ethanol (1 mL) and used for further estimations. The curcumin concentrations were measured spectrophotometrically at 425 nm.

Curcumin loading efficiency (*LE*) was calculated using the following equation:

$$LE(\%) = \frac{\text{Total curcumin content in NPs}}{\text{Total curcumin amount}} \times 100\%$$

Curcumin loading capacity (*LC*) in the preparations was calculated using the following equation:

$$LC(\%) = \frac{\text{Curcumin content}}{\text{Weight of nanoparticles}} \times 100\%$$

2.3. Curcumin In Vitro Release Study

2.3.1. Curcumin Release in PBS Solution

The curcumin in vitro release profile from the PVP-Cur NPs was obtained using dialysis technique as described [48]. PVP-Cur NPs were resuspended in 5 mL of PBS (pH 7.4) and dialyzed using Thermo Fisher Scientific (Waltham, MA, USA) tubes with a molecular weight cut-off (MWCO) of 1000 Da. During dialysis, the tubes were placed in a glass with 150 mL of PBS and incubated at 37 °C under constant shaking. The amount of curcumin released from PVP-Cur NPs was estimated by taking out 1.0 mL of buffer media at predetermined time intervals (0.5, 1, 2, 3, 4, 6, 8, 10, 12, 16, 20, 24, 36, 48 h). The content of the released curcumin in selected samples was determined by spectrophotometry at 425 nm. Free curcumin dissolved in methanol/water mixture at the same amount as in PVP-Cur NPs was used as a control. All samples' measurements were run in triplicate. The standard curcumin calibration curve was obtained and used as a reference in the experiments.

2.3.2. In Vitro Curcumin Release in Simulated Gastric, Intestinal and Colonic Digestion

In vitro curcumin release from PVP-Cur NPs was estimated as described by the authors in [49] using simulated gastric fluid (SGF, pH = 1.2) without enzymes (0.2% Polysorbate 80) for 2 h, simulated intestinal fluid (SIF, pH = 6.8) without enzymes (0.2% Polysorbate 80) for 6 h and simulated colonic fluid (SCF, pH = 7.4) (0.2% Polysorbate 80) with β-Galactosidase (0.13 units/mL) for 24 h at constant shaking and at 37 °C. Release medium was centrifuged, and the absorbance was measured spectrophotometrically at 425 nm to determine the amount of the released curcumin. All samples' measurements were run in triplicate.

2.3.3. Stability Studies

Stability characteristics of PVP-Cur NPs were evaluated according to the International Council for Harmonisation of Technical Requirements for Pharmaceuticals for Human Use (ICH) guidelines (2003) code Q1A(R2) (stability testing of new drug substances and products). Nanoparticle samples were stored preserved from light in closed impenetrable tubes. For the accelerated condition experiment, samples were taken at 0, 1, 2, 4 and 6 months (40 ± 2 °C, 75% relative humidity ± 5%). The amount of curcumin released from the samples was measured using a UV-Vis spectrophotometer (UNICO 2804, United Products & Instruments Inc., Dayton, NJ, USA) at 425 nm.

2.3.4. Water Resuspendability Study

Freeze-dried PVP-Cur NPs samples (10 mg) were dispersed in 10 mL of distilled water) and stirred for 5 min to test the homogeneity of the obtained suspensions using Zetasizer Nano Z&S (Malvern Instruments, Worcestershire, UK).

2.4. In Vitro and In Vivo Assays

2.4.1. Cell Lines

A431 epidermoid carcinoma cells (ATCC no. CRL-1555™) were cultured in DMEM with 4 mM L-glutamine supplemented with 10% FBS. Human embryonic kidney cells HEK 293 (ATCC no. CRL-1573™) were cultured in Eagle's Minimum Essential Medium,

and human glioblastoma cell lines T98G (ATCC no. CRL-1690TM) and U87 (ATCC no. HTB-14TM) were cultivated in Dulbecco's Modified Eagle Medium (DMEM) with 2 mM glutamine supplemented with 10% FBS. Cells were cultured at 37 °C in 5% CO₂ in a humidified atmosphere. All cells were passaged with 0.25% *v/w* trypsin—0.53 mM EDTA at 80% confluence.

Mouse embryonic fibroblasts NIH/3T3 cells (ATCC no. CRL-1658TM) were chosen as a control healthy cell line. NIH/3T3 were cultured in DMEM supplemented with 10% FBS, l-glutamine (1 mM) and penicillin–streptomycin (100 U/mL). Cells were incubated at 37 °C in a humidified atmosphere containing 5% CO₂ and split every 3 days using EDTA solution.

2.4.2. Cytotoxicity Assay

The three cell lines (NIH/3T3, T98G and U87) were used in the cytotoxicity assay.

Viability of cells was estimated by measuring activity of mitochondrial NAD(P)H-dependent cellular oxidoreductase enzymes which could reduce a yellow tetrazolium salt ((3-(4,5-dimethyl-2-thiazolyl)-2,5-diphenyl-2-H-tetrazolium bromide or MTT) to a violet formazan dye by metabolically active cells.

Cells were seeded in a 96-well plate in the amount of 8×10^3 cells per well. After overnight incubation, the studied substances (PVP, curcumin, PVP-Cur NPs) were added to cells in various concentrations in 100 µL of culture medium. After 24 h of drug exposition, cells were treated with 20 µL of MTT solution (MTT Cell Viability Assay Kit, Servicebio, Wuhan, China). In parallel, MTT was added to the wells with DMEM with NPs without cells that were used further for optical compensation. Incubation with MTT lasted for 4 h, then the medium was aspirated from the wells and formazan crystals were dissolved in dimethyl sulfoxide (DMSO). The compensation for DMSO absorbance was also performed. Optical density was measured at 570 nm on a Tecan Infinite[®] M Nano + spectrophotometer (Männedorf, Switzerland). Absorption values were converted to percentages relative to absorption values of intact cells.

2.4.3. Cell Uptake Assay

Cell uptake assay was performed on A431 and HEK 293 cell lines according to our previous work [27]. Briefly, the cells were seeded in a 96-well polystyrene plate at a density of 5×10^3 cells per well. After 24 h, the cells were washed with PBS and then preincubated for 15 min with Hoechst 33258 dissolved in the cell medium at a ratio of 1:1000 and then washed with the medium. After that, 150 µL of DMEM supplemented with either free curcumin or with the PVP-Cur NPs was added to the wells. To analyze the distribution of curcumin, the cells were washed three times with PBS and then visualized using a Zeiss Axio Observer.Z1 inverted microscope (Oberkochen, Germany).

2.4.4. Fish Embryo Acute Toxicity Test (FET)

Studies were conducted on zebrafish (*Danio rerio*) in accordance with OECD guideline Protocol 236 “Fish Embryo Acute Toxicity (FET) Test” (OECD/OCDE, 2013). Morphological effects were assessed according to [50].

Adult wild-type zebrafish were kept in aquariums with an aeration and recirculation system at a temperature of 28 °C, pH 6.5–7.5, with a photoperiod cycle of 14:10 h (light: dark). The fish were fed twice daily according to conventional recommendations (using zebrafish food).

Freshly laid eggs after fertilization (less 1 h post-fertilization (hpf)) were collected and placed in *Danio rerio* E3 embryo water (5 mM NaCl, 0.33 mM CaCl₂, 0.33 mM MgSO₄·7H₂O and 0.17 mM KCl and 0.1% methylene blue). Unfertilized eggs and embryos that had significant developmental defects 24 h after fertilization were detected under a Nexcope NSZ-810 microscope (Ningbo, China) and removed from the experiment. Experimental embryos were mechanically dechorionized with tweezers and placed in 24-well plates (2 embryos per well, total 0.5–1.5 mL of solution per well). PVP-Cur NPs nanoparticles were

added in quantities such that final concentrations ranged from 0.1 to 100 μM of curcumin in each well. Each well procedure was performed in triplicate ($n = 6$ per group).

The embryos were examined 24 (48 hpf) and 72 (96 hpf) hours after the addition of nanoparticles. Developmental disorders and delays and morphological changes, including irregular shape of the yolk sacs, impaired tail development, and decreased motor activity, were recorded.

To estimate the full range of mortality from 0 to 100%, embryonic deaths were recorded at 24 (48 hpf) and 72 (96 hpf) hours after addition of compounds. Toxicity assay (LC_{50} calculation) was determined based on cumulative mortality at the end of the experiment and was estimated using regression analysis.

2.5. Statistical Analysis

In cytotoxicity studies, the obtained data represented a normal distribution. The experiments were performed for no less than three times in three replicates. Statistical analysis was conducted using ordinary one-way ANOVA followed by Dunnett's multiple comparisons test using Graphpad Prism 6.01 software (San Diego, CA, USA).

3. Results

3.1. Physicochemical Characteristics of PVP-Cur NPs

The basic properties, size, shape and ζ -potential of the PVP-Cur NPs were determined after resuspension of the resulting samples in water. The water resuspendability test showed that freeze-dried PVP-Cur NPs samples were easily dispersed back into distilled water and appeared translucent, similar to original nanoparticle dispersion before freeze-drying, which was confirmed by the results of the dynamic light scattering (DLS) analysis. All basic properties before and after freeze-drying are shown in Table 1.

Table 1. The main characteristics of the nanoparticles before and after freeze-drying.

PVP-Cur NPs	Z-Average Hydrodynamic Diameter (nm \pm SD)	LC (% Mass \pm SD)	LE (% Mass \pm SD)	ζ -Potential (mV \pm SD)
Before freeze-drying	191.1 \pm 11.3	9.3 \pm 0.3	93.9 \pm 1.2	−4.00 \pm 0.41
After freeze-drying	190.0 \pm 12.2	9.2 \pm 0.5	93.6 \pm 1.1	−4.21 \pm 0.15

Given that the loading of curcumin was about 10 wt.% of the polymer mass, the degree of encapsulation of biologically active substances in nanoparticles reached 95%.

The PVP-Cur NPs were spherical particles, as shown by TEM (Figure 1A,B) and AFM (Figure 1C). For the AFM imaging, NPs were deposited onto TEM grids (amorphous carbon) rather than mica or graphite, which are commonly used as substrates. We chose the grids treated with the glow discharge because the adsorption of the NPs onto their surface was relatively high, and they were previously used as substrates for the AFM imaging [51].

The size of the NPs was measured using TEM, AFM and DLS, and the obtained data are summarized in Figure 1E.

The z-average size and the number average measured using DLS (190 nm and 150 nm, respectively (Figure 1D,E)) were higher than the mean particle size determined using microscopy. This is the difference between the particle hydrodynamic diameter measured by DLS and the particle projection diameter assessed by the AFM and TEM. A similar difference was observed for the poly(styrene-co-acrylic acid) copolymer particles [52]. The mean polydispersity index (*PDI*) of the NPs was 0.10 ± 0.03 by DLS, which confirms the homogeneity of the analyzed NPs. The *PDI* based on the TEM data can be easily calculated by the following formula:

$$PDI = \left(\frac{SD}{\text{mean diameter}} \right)^2$$

where *SD* is the standard deviation.

In our case, according to the TEM data, $SD = 40$ nm and mean diameter = 118 nm, so we obtained an estimate for PDI of ~ 0.11 , which is in agreement with the value obtained using DLS.

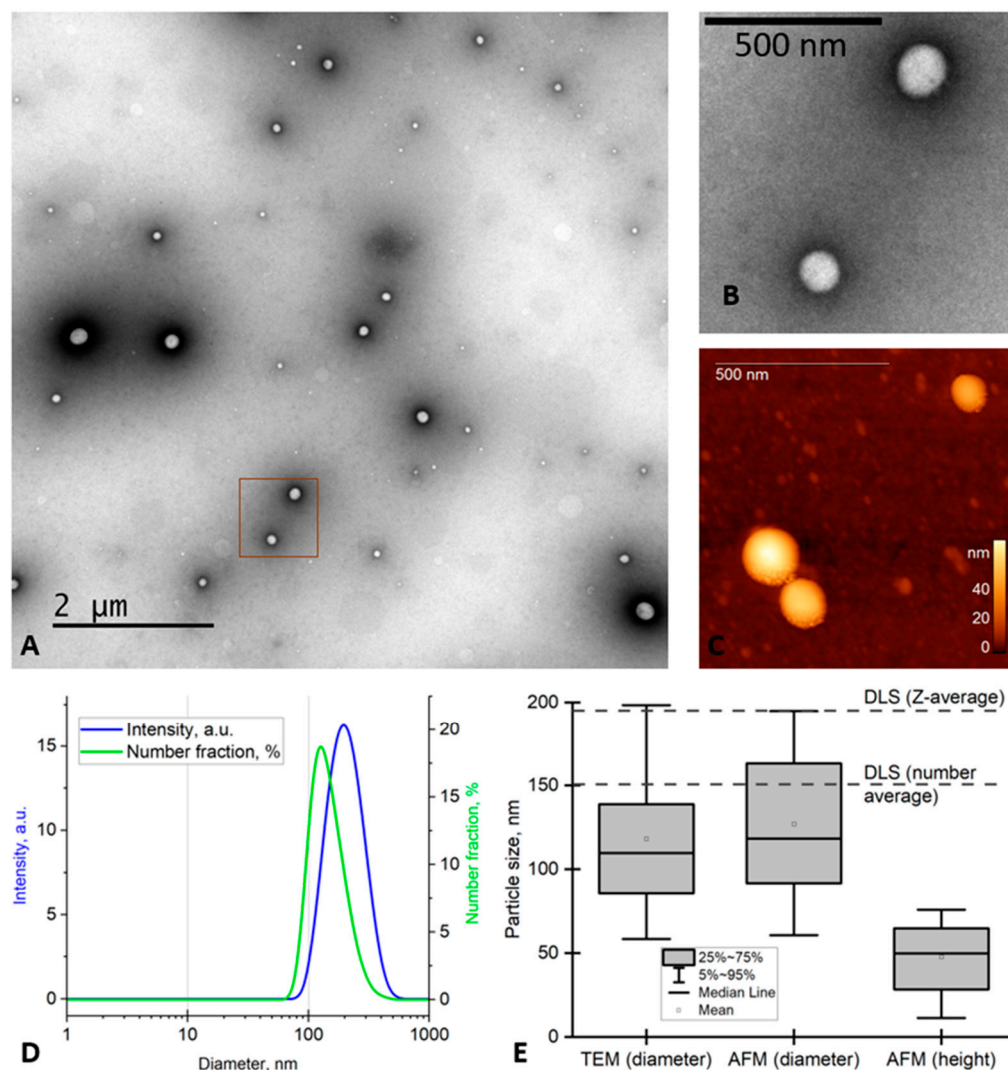


Figure 1. Characterization of the PVP-Cur NPs using TEM (A,B), AFM (C) and DLS (D) and the measured sizes (E). The image B shows the magnified part of image A. The dotted lines in E show the z-average and the number average obtained using DLS.

Overall, the data obtained using the single-particle measurements (AFM, TEM) and ensemble measurements (DLS) were in good agreement.

3.2. Curcumin In Vitro Release Study

PVP-Cur NPs were incubated at 37 °C in PBS; the in vitro release profile studied over 48 h is presented as a cumulative release percentage in Figure 2A.

As one can see, a typical two-phase release profile was observed for the tested formulation when it was placed to the released medium. First, there was a relatively rapid release of about 10% of the loaded curcumin in the initial 30 min, followed by sustained release of the remaining curcumin by 24 h. In comparison, over 30% of the curcumin from the control water/methanol mixture was released into the medium rapidly by 30 min, with further almost complete curcumin recovery after 3 h.

The in vitro curcumin release study has been designed to simulate the human digestion tracks. The resulting curve of cumulative curcumin release from PVP-Cur NPs is presented in Figure 2B.

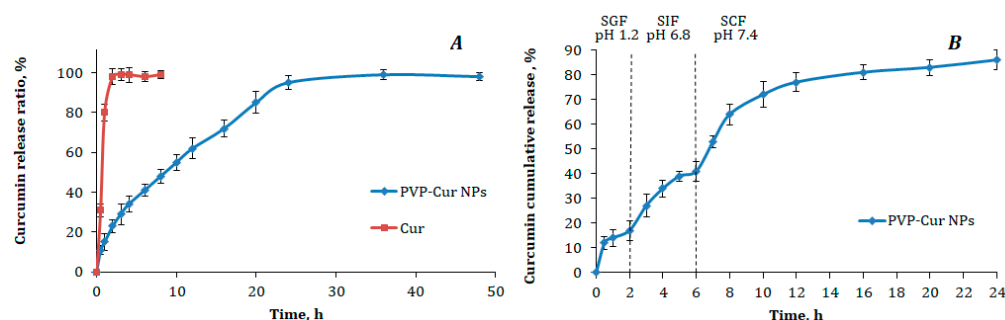


Figure 2. (A) Curcumin in vitro release profiles from PVP-Cur NPs and curcumin solution (Cur) in PBS (pH 7.4) at 37 °C; (B) cumulative curcumin release from the PVP-Cur NPs into simulated gastric fluids modeling three digestive system tracts. Data are plotted as the average \pm SD of three measurements.

In the first medium, which simulated gastric fluid (pH 1.2) similarly to the abovementioned experiment, there was observed a slight burst effect, which can be explained mostly by the release of curcumin bound to the PVP outer shell. With the increase of the pH value of the media in simulated intestinal fluid (pH 6.8) and simulated colonic fluid (pH 7.4), higher curcumin amounts were released in a sustainable manner. The steps after 2 h and 6 h of the experiment were caused by the switch of the release media. The cumulative drug release for 24 h from the PVP-Cur NPs was about 85%. It can also be mentioned that only a rather small amount of curcumin was released into the fluid modeling the stomach's acidic environment, while the highest amount of curcumin was released into the simulated colonic fluid.

During the stability test, no changes were observed in the content of curcumin in PVP-Cur NPs or in their average size in the accelerated stability studies (Table 2), which is evidence of rather good stability of the obtained PVP-Cur NPs.

Table 2. Accelerated stability studies of PVP-Cur NPs according to the ICH guidelines.

Time (Month)	Residual Curcumin Content (%)	Average Size (nm \pm SD)
0	100.00	190.0 \pm 12.3
1	99.04	191.2 \pm 13.3
2	97.23	189.5 \pm 12.8
4	96.62	190.4 \pm 12.9
6	94.11	190.3 \pm 13.7

3.3. Cytotoxicity Assay

The cytotoxicity of PVP-Cur NPs in comparison with curcumin and PVP was studied in glioblastoma cell lines T98G and U87 (Figure 3A,B). Normal NIH/3T3 mouse embryonic fibroblasts were used as control (Figure 3C). The viability of fibroblast cells exceeded 85% for free curcumin and PVP-Cur. Viability was above 85% for free PVP. The half-maximal inhibition concentration (IC_{50}) of curcumin was $70.1 \pm 3.5 \mu\text{M}$ for T98G cells and $48.6 \pm 1.7 \mu\text{M}$ for U87 cells. The IC_{50} of PVP-Cur NPs was determined to be $29.3 \pm 3.7 \mu\text{M}$ and $20.7 \pm 1.3 \mu\text{M}$ for T98G and U87 cells, respectively.

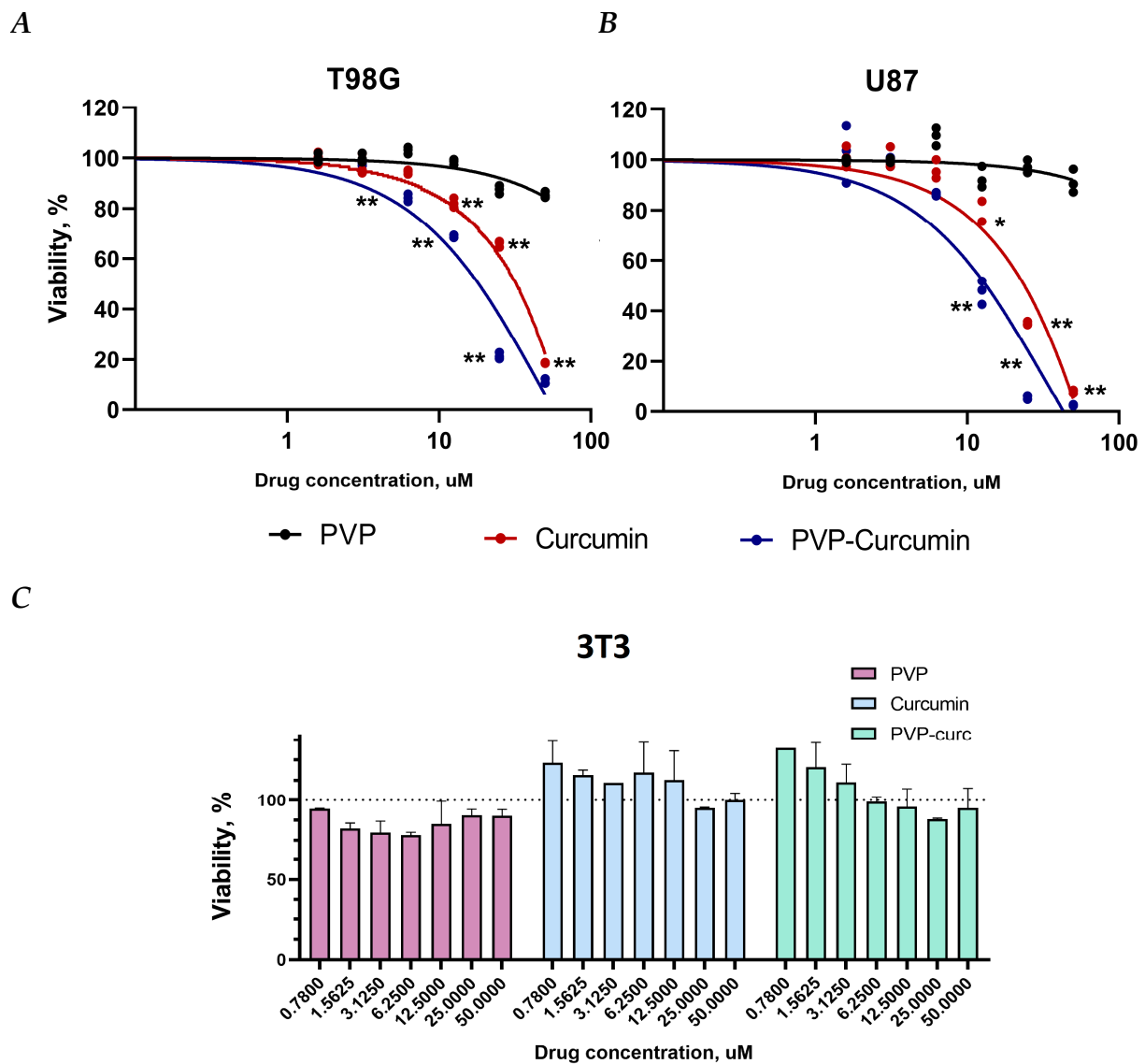


Figure 3. Cytotoxicity of PVP-Cur NPs, curcumin and PVP in (A) T98G, (B) U87 and (C) 3T3 cells. The data were analyzed using Graphpad Prism 6.01 software. Statistical analysis was performed using ordinary one-way ANOVA followed by Dunnett's multiple comparisons test using Graphpad Prism 6.01 software (San Diego, CA, USA). * $p < 0.05$ and ** $p < 0.005$ indicate significant differences from the control.

3.4. Cell Uptake Assay

PVP-Cur NPs were used for in vitro uptake studies in A431 epidermoid carcinoma and HEK293 human embryonic kidney cells. Relative fluorescence intensities were compared 60 min after cells were treated with NPs and free curcumin. Sixty minute after treating cells with free curcumin and PVP-Cur NPs, it was shown that the relative fluorescence intensity of curcumin loaded into the nanoparticles was 1.5 times higher than that of the free curcumin (Figure 4). This difference in the absorption is due to the presence of an amphiphilic poly(N-vinylpyrrolidone) shell and correlates with other studies related to curcumin encapsulation [53,54].

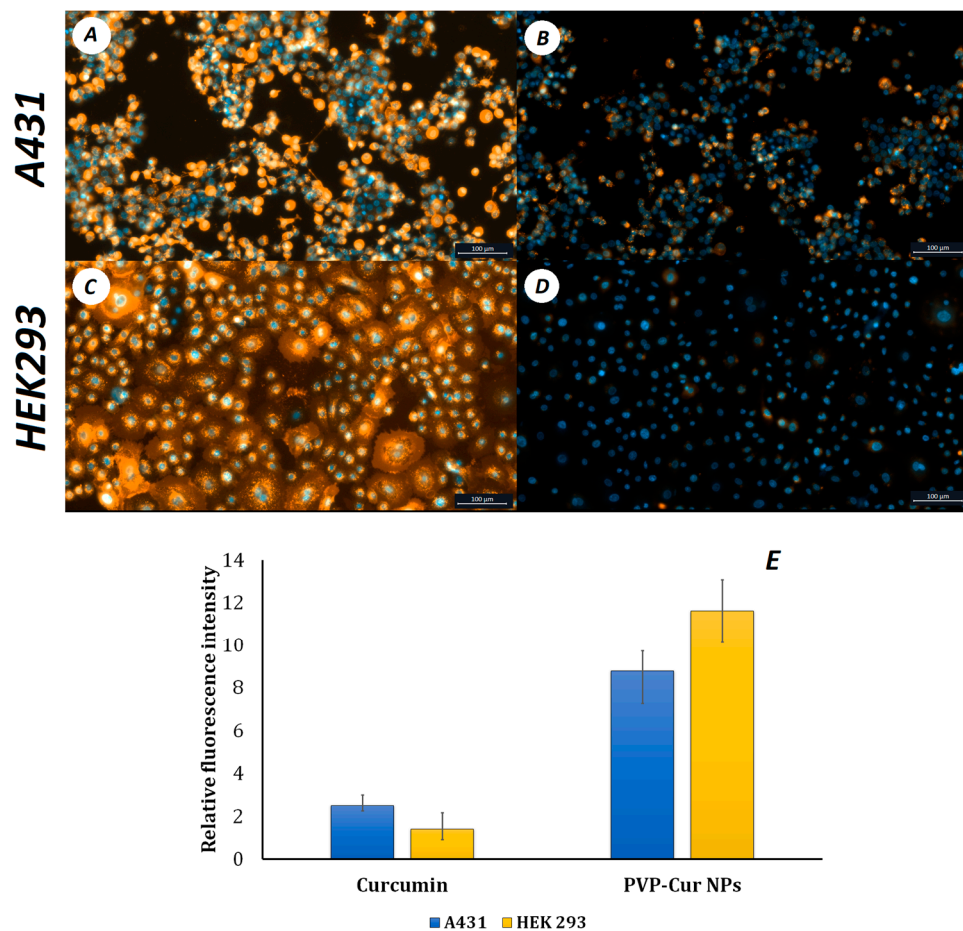


Figure 4. Uptake of PVP-Cur NPs (A,C) and free curcumin (B,D) by A431 and HEK 293 cells and relative fluorescence intensity after 60 min (E).

3.5. Fish Embryo Acute Toxicity Test (FET)

Zebrafish embryo treatment with PVP-Cur NPs in concentrations 25, 50 and 100 μM provided neurotoxicity that was characterized by increased motor activity of the tail (Figure 5).

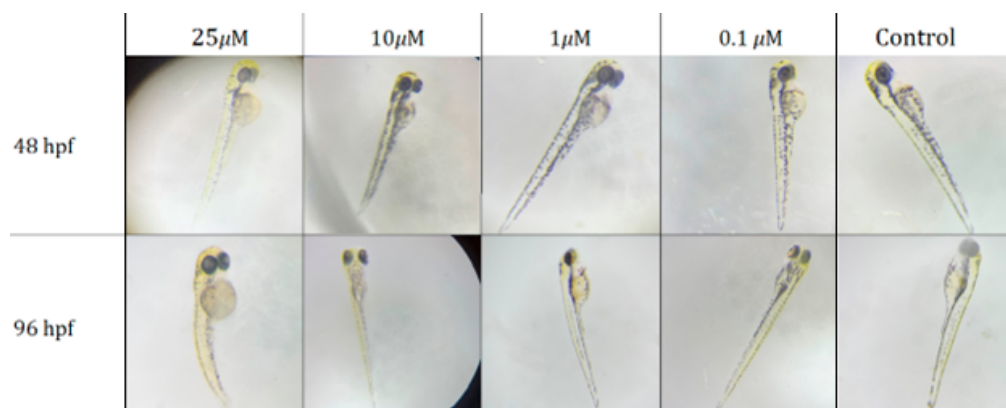


Figure 5. *Danio rerio* embryos aged 48 and 96 hpf after 24 h (48 hpf) and 72 h (96 hpf) of incubation with the studied curcumin nanoparticles at 40 \times magnification.

The death of all embryos was observed after 24 h of treatment with nanoparticles in concentrations of 50 and 100 μM per PVP-Cur NPs. Embryos that were treated with concentration of 25 μM had enlargement of the yolk sac and developmental delay after

24 h, which persisted 72 h after incubation, and 5 out of 6 embryos were found dead in 72 h of experiments. Concentrations of 10, 1 and 0.1 μM provided no toxic effects. The LC_{50} value was determined as 23.7 μM (Figure 6).

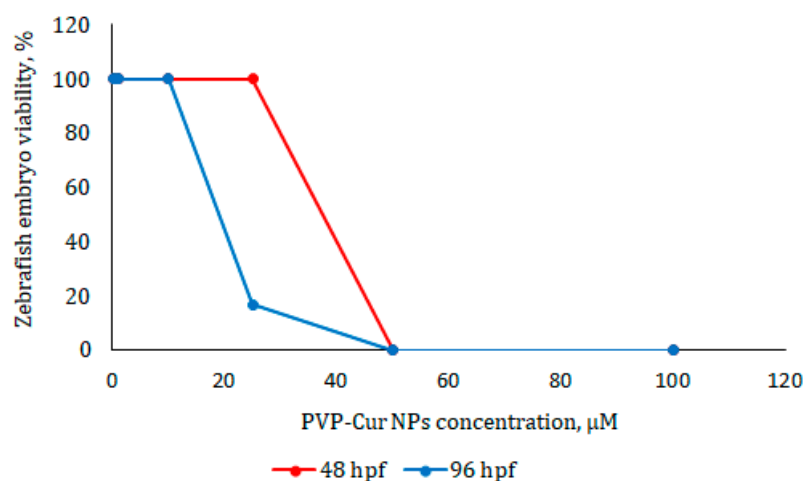


Figure 6. Survival of *Danio rerio* embryos ($n = 6$ per group) during 24 h (48 hpf) and 72 h (96 hpf) incubation with PVP-Cur NPs. Lethal concentration $\text{LC}_{50} = 23.7 \mu\text{M}$ (per curcumin contents) was determined by regression analysis using Graphpad Prism version 6.01.

4. Discussion

We have previously shown the possibility of using amphiphilic PVPs with different molecular weights as drug carriers. In this work, we show that amphiphilic poly(N-vinylpyrrolidone) may be a suitable curcumin carrier for cancer treatment.

Amphiphilic poly(N-vinylpyrrolidone) was synthesized by radical polymerization. The molecular weight of the resulting polymer was 6 kDa. As it was shown previously, this molecular weight accounts for suitable critical aggregation concentration and low toxicity of the polymer [21,25,27]. PVP-Cur NPs were obtained by the solvent evaporation method: dispersion was carried out using an ultrasonic homogenizer using two infinitely compatible solvents (acetone/water). The samples obtained by this method have an average hydrodynamic diameter of about 200 nm as determined by DLS. It has been established that the ζ -potential ranges from -4 to -5 mV and differs little from the ζ -potential of the outer cell membrane, which also has a close negative value and can range from -2 to -90 mV depending on the cell type, the composition of a particular membrane region and the pH of the environment [55,56]. It should be noted that the electrical stabilization of low-molecular-weight surfactants is reflected by high absolute surface charge values, while for high-molecular-weight surfactants (i.e., amphiphilic polymers), stabilization is achieved through different mechanisms (i.e., steric stabilization) and is not clearly reflected by the absolute value of the surface charge [57].

The mean diameter of the particles was 118 ± 40 nm and 127 ± 41 nm (mean \pm SD) according to TEM and AFM, respectively. The latter diameter was higher due to the AFM tip broadening. The height of the particles above the substrate (48 ± 40 nm) was far smaller than their lateral diameter, and the difference indicates intense flattening of the particles. Additionally, it can be a consequence of the variations in the tip-sample interaction, which shifts the cantilever resonance frequency [58]. A similar difference between the height and width measured using AFM was previously observed for viruses [59,60], polymer nanoparticles [23], DNA [61] and other samples.

As curcumin is a poorly water soluble and dispersible substance, its encapsulation strategy using polymeric micelle-like nanoparticles was studied and revealed as a successful way to improve this essential physicochemical property.

The prepared NPs showed favorable long-term stability. This improvement could be explained by the unique core-shell structure of polymeric micelle-like aggregates immo-

bilizing curcumin as hydrophobic cargo in their hydrophobic inner core, while the PVP hydrophilic shell contributes to solubilizing of these nanoparticles in the aqueous media.

In current study PVP-Cur NPs showed an *in vitro* two-phase release profile in PBS (pH 7.4), composed of an immediate drug release followed by a sustained release. The two-phase delivery system helps in overcoming multiple dosing regimen problems. The initial burst release can be caused by the release of the drug entrapped in the polymeric shell of the nanoparticles, whereas the sustained release is the result of the drug diffusion from the hydrophobic core of the nanoparticles. Moreover, the outer shell PVP layer probably forms a diffusion obstacle for the released drug, resulting in a slower release. Therefore, obtained results imply that the release profile of the studied nano-scaled carrier systems is significantly affected both by hydrophobic interactions in the nanoparticle core and by the polymer coating layer.

The *in vitro* curcumin release investigation in simulated gastric fluids with a sequence of pH values of 1.2, 6.8 and 7.4 revealed that a low amount of curcumin release occurs at pH 1.2 and 6.8, while an increased extent of sustained release is discovered at pH 7.4.

The release profile shows sustained slow, gradual release of curcumin at each point of time from polymeric nanoparticles at a physiologic pH of 7.4. Sustained drug release from the nanoparticles is an important feature as it can dramatically increase the biologically active substance bioavailability and prolong diagnostic or therapeutic effect.

Curcumin obtains multiple effects *in vivo*, including antiproliferative, anti-inflammatory and antioxidant effects [62], which suggests that it can be utilized as a component of anti-cancer therapy. However, curcumin obtains poor stability *in vitro* and *in vivo* with a half-life of about 5 min, preventing it from exhibiting any therapeutically relevant effects [63]. Therefore, encapsulating curcumin into nanoparticles helps improve its bioavailability and ensures delivery to the lesion site, where it can exert its therapeutic properties.

In the current study, cytotoxicity assays showed that PVP-Cur NPs are non-toxic for healthy fibroblasts. Previously, the low cytotoxicity of PVP NPs, including those with curcumin, was shown for different cell types, including human embryonic stem cell derived fibroblasts (EBF-H9), human microvascular endothelial cells (HMEC-1), human embryonic kidney cells (HEK 293) and others [43,57,64–66].

The cell uptake assay showed that curcumin encapsulated in core/shell PVP-Cur NPs is transferred into the intracellular space 1.5 times more effectively than free curcumin. This difference in absorption is due to the presence of an amphiphilic poly(N-vinylpyrrolidone) shell, which is similar to liposome shells and correlates with other studies related to curcumin encapsulation. The mechanism of action is similar to the interaction of liposomes with cells. This is why the fluorescence of curcumin in cells is higher in the case of PVP-Cur NPs than in the case of free curcumin [67–69].

Due to accelerated cellular uptake of nanoparticles *in vitro*, the toxicity of PVP-Cur NPs increased compared to free curcumin against malignant cancer cells. This is consistent with the data previously obtained in [70]. Numerous studies demonstrate that curcumin can target signaling pathways involved in glioblastoma development: for example, by modulating the activity of transcription factors such as NF- κ B and STAT3 and regulating the expression of genes implicated in malignant transformation and cell survival [71–73]. Curcumin is shown to modulate properties of glioblastoma stem cells via activation of autophagy [74]. Also, curcumin was reported to enhance the effect of radiation on glioma cells [75], making it a potential candidate for treatment of this type of cancer.

It can be assumed that such nanoparticles loaded with curcumin will be suitable for the treatment of malignant cancers, in particular glioblastoma. *In vivo* acute toxicity results on zebrafish indicated that below a concentration of 23.7 μ M, PVP-Cur NPs are safe for use in living organisms.

5. Conclusions

Curcumin-loaded nanoparticles based on amphiphilic poly(N-vinylpyrrolidone) were synthesized in this study. The molecular weight of PVP was 6 kDa and was the most

suitable due to its hydrophilic–hydrophobic balance. PVP-Cur NPs obtained by the solvent evaporation method had spherical form, an average hydrodynamic diameter of about 200 nm and the ζ -potential was between -4 and -5 mV. PVP-Cur NPs are non-toxic for healthy fibroblast cells and very toxic for glioblastoma cells. The IC_{50} of PVP-Cur NPs was determined to be 29.3 ± 3.7 μ M and 20.7 ± 1.3 μ M for T98G and U87 cells, respectively. In vivo experiments on zebrafish shows that PVP-Cur NPs do not have acute toxicity at concentrations below 23.7 μ M. The in vitro release profiles in different media indicate that amphiphilic PVP nanoparticles have prolonged release action and can be considered as a prospective drug delivery system. Overall, the PVP-Cur NPs are promising for the treatment of malignant cancers without toxic effects for healthy cells and organs.

Author Contributions: Conceptualization—A.N.K. and A.L.L.; Methodology—D.V.B., V.S.P. and A.V.Y.; Validation—A.V.Y. and I.I.K.; Formal analysis—D.A.D. and M.E.G.; Investigation, E.V.K., M.V.S., I.I.K. and V.S.P.; Writing—original draft, A.L.L. and A.N.K.; Writing—review & editing, D.V.B., M.E.G. and A.V.Y.; Visualization—M.V.S., A.N.K. and A.L.L.; Project administration, A.N.K. and D.A.D. All authors have read and agreed to the published version of the manuscript.

Funding: This work was financially supported by the Russian Science Foundation, grant No. 23-15-00468, <https://rscf.ru/project/23-15-00468/> (accessed on 13 November 2023).

Institutional Review Board Statement: The study was conducted in accordance with the European Convention for the Protection of Vertebrate Animals Used for Experimental and Other Scientific Purposes (CETS No. 123) and the protocol was approved by the Ethics Committee of N.N. Blokhin National Medical Research Centre for Oncology (Protocol 03p, 16 May 2023).

Informed Consent Statement: Not applicable.

Data Availability Statement: All data are publicly available via open access on journal website. Additional data are available upon request.

Acknowledgments: The TEM measurements were performed at the User Facilities Center «Electron Microscopy in the Life Sciences» at Lomonosov Moscow State University.

Conflicts of Interest: The authors declare no conflict of interest.

References

1. D'souza, A.A.; Shegokar, R. Polyethylene glycol (PEG): A versatile polymer for pharmaceutical applications. *Expert Opin. Drug Deliv.* **2016**, *13*, 1257–1275. [[CrossRef](#)] [[PubMed](#)]
2. Suk, J.S.; Xu, Q.; Kim, N.; Hanes, J.; Ensign, L.M. PEGylation as a strategy for improving nanoparticle-based drug and gene delivery. *Adv. Drug Deliv. Rev.* **2016**, *99*, 28–51. [[CrossRef](#)] [[PubMed](#)]
3. Shi, D.; Beasock, D.; Fessler, A.; Szebeni, J.; Ljubimova, J.Y.; Afonin, K.A.; Dobrovolskaia, M.A. To PEGylate or not to PEGylate: Immunological properties of nanomedicine's most popular component, polyethylene glycol and its alternatives. *Adv. Drug Deliv. Rev.* **2022**, *180*, 114079. [[CrossRef](#)] [[PubMed](#)]
4. Tyler, B.; Gullotti, D.; Mangraviti, A.; Utsuki, T.; Brem, H. Polylactic acid (PLA) controlled delivery carriers for biomedical applications. *Adv. Drug Deliv. Rev.* **2016**, *15*, 163–175. [[CrossRef](#)] [[PubMed](#)]
5. Casalini, T.; Rossi, F.; Castrovinci, A.; Perale, G. A Perspective on Poly(lactic Acid)-Based Polymers Use for Nanoparticles Synthesis and Applications. *Front. Bioeng. Biotechnol.* **2019**, *7*, 259. [[CrossRef](#)]
6. Na, Y.; Zhang, N.; Zhong, X.; Gu, J.; Yan, C.; Yin, S.; Lei, X.; Zhao, J.; Geng, F. Poly(lactic-co-glycolic acid)-based nanoparticles modified with peptides and other linkers cross the blood-brain barrier for targeted drug delivery. *Nanomedicine* **2023**, *18*, 125–143. [[CrossRef](#)]
7. Rocha, C.V.; Gonçalves, V.; da Silva, M.C.; Bañobre-López, M.; Gallo, J. PLGA-Based Composites for Various Biomedical Applications. *Int. J. Mol. Sci.* **2022**, *23*, 2034. [[CrossRef](#)]
8. Liu, C.; Zhang, S.; McClements, D.J.; Wang, D.; Xu, Y. Design of Astaxanthin-Loaded Core-Shell Nanoparticles Consisting of Chitosan Oligosaccharides and Poly(lactic-co-glycolic acid): Enhancement of Water Solubility, Stability, and Bioavailability. *J. Agric. Food Chem.* **2019**, *67*, 5113–5121. [[CrossRef](#)]
9. Mohammadian, S.; Khazaei, M.; Maghami, P.; Avan, A.; Rezaei, M. Polycaprolactone-based Nanocarriers Containing 5-fluorouracil as a Therapeutic Guided Drug Delivery Approach for Enhancing Anticancer Activity. *Curr. Cancer Drug Targets* **2023**, *23*, 524–533. [[CrossRef](#)]
10. Pohlmann, A.R.; Fonseca, N.F.; Paese, K.; Detoni, C.B.; Coradini, K.; Beck, R.C.; Guterres, S.S. Poly(ϵ -caprolactone) microcapsules and nanocapsules in drug delivery. *Expert Opin. Drug Deliv.* **2013**, *10*, 623–638. [[CrossRef](#)]

11. Franco, P.; De Marco, I. The Use of Poly(N-vinyl pyrrolidone) in the Delivery of Drugs: A Review. *Polymers* **2020**, *12*, 1114. [[CrossRef](#)] [[PubMed](#)]
12. Waleka, E.; Stojek, Z.; Karbarz, M. Activity of Povidone in Recent Biomedical Applications with Emphasis on Micro- and Nano Drug Delivery Systems. *Pharmaceutics* **2021**, *13*, 654. [[CrossRef](#)] [[PubMed](#)]
13. Luo, Y.; Hong, Y.; Shen, L.; Wu, F.; Lin, X. Multifunctional Role of Polyvinylpyrrolidone in Pharmaceutical Formulations. *AAPS PharmSciTech* **2021**, *22*, 34. [[CrossRef](#)] [[PubMed](#)]
14. Moffitt, E.A. Blood substitutes. *Can. Anaesth. Soc. J.* **1975**, *22*, 12–19. [[CrossRef](#)] [[PubMed](#)]
15. Bigliardi, P.L.; Alsagoff, S.A.L.; El-Kafrawi, H.Y.; Pyon, J.-K.; Wa, C.T.C.; Villa, M.A. Povidone iodine in wound healing: A review of current concepts and practices. *Int. J. Surg.* **2017**, *44*, 260–268. [[CrossRef](#)] [[PubMed](#)]
16. Malet, F.; Karsenti, D.; Pouliquen, P. Preservative-free ocular hydrating agents in symptomatic contact lens wearers: Saline versus PVP solution. *Eye Contact Lens* **2003**, *29*, 38–43. [[CrossRef](#)]
17. Inactive Ingredient Search for Approved Drug Products. Available online: <https://www.accessdata.fda.gov/scripts/cder/iig/index.cfm> (accessed on 15 September 2023).
18. Kulikov, P.P.; Luss, A.L.; Nelemans, L.C.; Shtilman, M.I.; Mezhuev, Y.O.; Kuznetsov, I.A.; Sizova, O.Y.; Christiansen, G.; Pennisi, C.P.; Gurevich, L. Synthesis, Self-Assembly and In Vitro Cellular Uptake Kinetics of Nanosized Drug Carriers Based on Aggregates of Amphiphilic Oligomers of N-Vinyl-2-pyrrolidone. *Materials* **2021**, *14*, 20. [[CrossRef](#)]
19. Kuskov, A.N.; Kulikov, P.P.; Goryachaya, A.V.; Tzatzarakis, M.N.; Docea, A.O.; Velonia, K.; Shtilman, M.I.; Tsatsakis, A.M. Amphiphilic poly-N-vinylpyrrolidone nanoparticles as carriers for non-steroidal, anti-inflammatory drugs: In vitro cytotoxicity and in vivo acute toxicity study. *Nanomedicine* **2017**, *13*, 1021–1030. [[CrossRef](#)]
20. Kuskov, A.N.; Voskresenskaya, A.A.; Goryachaya, A.V.; Shtilman, M.I.; Spandidos, D.A.; Rizos, A.K.; Tsatsakis, A.M. Amphiphilic poly-N-vinylpyrrolidone nanoparticles as carriers for non-steroidal anti-inflammatory drugs: Characterization and in vitro controlled release of indomethacin. *Int. J. Mol. Med.* **2010**, *26*, 85–94.
21. Kuskov, A.; Nikitovich, D.; Berdiaki, A.; Shtilman, M.; Tsatsakis, A. Amphiphilic Poly-N-vinylpyrrolidone Nanoparticles as Carriers for Nonsteroidal, Anti-Inflammatory Drugs: Pharmacokinetic, Anti-Inflammatory, and Ulcerogenic Activity Study. *Pharmaceutics* **2022**, *14*, 925. [[CrossRef](#)]
22. Artyukhov, A.A.; Nechaeva, A.M.; Shtilman, M.I.; Chistyakov, E.M.; Svistunova, A.Y.; Bagrov, D.V.; Kuskov, A.N.; Docea, A.O.; Tsatsakis, A.M.; Gurevich, L.; et al. Nanoaggregates of Bipphilic Carboxyl-Containing Copolymers as Carriers for Ionically Bound Doxorubicin. *Materials* **2022**, *15*, 7136. [[CrossRef](#)] [[PubMed](#)]
23. Yamskov, I.A.; Kuskov, A.N.; Babievsky, K.K.; Berezin, B.B.; Krayukhina, M.A.; Samoylova, N.A.; Tikhonov, V.E.; Shtilman, M.I. Novel liposomal forms of antifungal antibiotics modified by amphiphilic polymers. *Appl. Biochem. Microbiol.* **2008**, *44*, 624–628. [[CrossRef](#)]
24. Yagolovich, A.; Kuskov, A.; Kulikov, P.; Kurbanova, L.; Bagrov, D.; Artykov, A.; Gasparian, M.; Sizova, S.; Oleinikov, V.; Gileva, A.; et al. Amphiphilic Poly(N-vinylpyrrolidone) Nanoparticles Conjugated with DR5-Specific Antitumor Cytokine DR5-B for Targeted Delivery to Cancer Cells. *Pharmaceutics* **2021**, *13*, 1413. [[CrossRef](#)] [[PubMed](#)]
25. Yagolovich, A.; Kuskov, A.; Kulikov, P.; Kurbanova, L.; Gileva, A.; Markvicheva, E. Antitumor Cytokine DR5-B-Conjugated Polymeric Poly(N-vinylpyrrolidone) Nanoparticles with Enhanced Cytotoxicity in Human Colon Carcinoma 3D Cell Spheroids. *Mater. Proc.* **2021**, *7*, 8.
26. Kuskov, A.; Selina, O.; Kulikov, P.; Imatdinov, I.; Balysheva, V.; Kryukov, A.; Shtilman, M.; Markvicheva, E. Amphiphilic Poly(N-Vinylpyrrolidone) Nanoparticles Loaded with DNA Plasmids Encoding Gn and Gc Glycoproteins of the Rift Valley Fever Virus: Preparation and In Vivo Evaluation. *ACS Appl. Bio Mater.* **2021**, *4*, 6084–6092. [[CrossRef](#)]
27. Luss, A.L.; Kulikov, P.P.; Romme, S.B.; Andersen, C.L.; Pennisi, C.P.; Docea, A.O.; Kuskov, A.N.; Velonia, K.; Mezhuev, Y.O.; Shtilman, M.I.; et al. Nanosized carriers based on amphiphilic poly-N-vinyl-2-pyrrolidone for intranuclear drug delivery. *Nanomedicine* **2018**, *13*, 703–715. [[CrossRef](#)]
28. Ganji, A.; Farahani, I.; Saeedifar, A.M.; Mosayebi, G.; Ghazavi, A.; Majeed, M.; Jamialahmadi, T.; Sahebkar, A. Protective Effects of Curcumin against Lipopolysaccharide-Induced Toxicity. *Curr. Med. Chem.* **2021**, *28*, 6915–6930. [[CrossRef](#)]
29. Barua, N.; Buragohain, A.K. Therapeutic Potential of Curcumin as an Antimycobacterial Agent. *Biomolecules* **2021**, *11*, 1278. [[CrossRef](#)]
30. Tomeh, M.A.; Hidianamrei, R.; Zhao, X. A Review of Curcumin and Its Derivatives as Anticancer Agents. *Int. J. Mol. Sci.* **2019**, *20*, 1033. [[CrossRef](#)]
31. Feltrina, F.d.S.; Agner, T.; Sayer, C.; Lona, L.M.F. Curcumin encapsulation in functional PLGA nanoparticles: A promising strategy for cancer therapies. *Adv. Colloid Interface Sci.* **2022**, *300*, 102582. [[CrossRef](#)]
32. Ataei, M.; Gumprich, E.; Kesharwani, P.; Jamialahmadi, T.; Sahebkar, A. Recent advances in curcumin-based nanoformulations in diabetes. *J. Drug Target.* **2023**, *31*, 671–684. [[CrossRef](#)] [[PubMed](#)]
33. Hartogh, D.J.D.; Gabriel, A.; Tsiani, E. Antidiabetic Properties of Curcumin I: Evidence from In Vitro Studies. *Nutrients* **2020**, *12*, 118. [[CrossRef](#)] [[PubMed](#)]
34. Chamani, S.; Moossavi, M.; Naghizadeh, A.; Abbasifard, M.; Majeed, M.; Johnston, T.P.; Sahebkar, A. Immunomodulatory effects of curcumin in systemic autoimmune diseases. *Phytother. Res.* **2022**, *36*, 1616–1632. [[CrossRef](#)] [[PubMed](#)]
35. Fridlender, M.; Kapulnik, Y.; Koltai, H. Plant derived substances with anti-cancer activity: From folklore to practice. *Front. Plant Sci.* **2015**, *6*, 799. [[CrossRef](#)] [[PubMed](#)]

36. Iqbal, J.; Abbasi, B.A.; Mahmood, T.; Kanwal, S.; Ali, B.; Shah, S.A.; Khalil, A.T. Plant-derived anticancer agents: A green anticancer approach. *Asian Pac. J. Trop. Biomed.* **2017**, *7*, 1129–1150. [[CrossRef](#)]
37. de Waure, C.; Bertola, C.; Baccarini, G.; Chiavarini, M.; Mancuso, C. Exploring the Contribution of Curcumin to Cancer Therapy: A Systematic Review of Randomized Controlled Trials. *Pharmaceutics* **2023**, *15*, 1275. [[CrossRef](#)] [[PubMed](#)]
38. Omidian, H.; Wilson, R.L.; Chowdhury, S.D. Enhancing Therapeutic Efficacy of Curcumin: Advances in Delivery Systems and Clinical Applications. *Gels* **2023**, *9*, 596. [[CrossRef](#)] [[PubMed](#)]
39. Banazadeh, M.; Behnam, B.; Ganjooei, N.A.; Gowda, B.H.J.; Kesharwani, P.; Sahebkar, A. Curcumin-based nanomedicines: A promising avenue for brain neoplasm therapy. *J. Drug Deliv. Sci. Technol.* **2023**, *89*, 105040. [[CrossRef](#)]
40. Anand, P.; Kunnumakkara, A.B.; Newman, R.A.; Aggarwal, B.B. Bioavailability of curcumin: Problems and promises. *Mol. Pharm.* **2007**, *4*, 807–818. [[CrossRef](#)]
41. Sanidad, K.Z.; Sukamtoh, E.; Xiao, H.; McClements, D.J.; Zhang, G. Curcumin: Recent Advances in the Development of Strategies to Improve Oral Bioavailability. *Annu. Rev. Food Sci. Technol.* **2019**, *10*, 597–617. [[CrossRef](#)]
42. Liu, C.; Yuan, Y.; Ma, M.; Zhang, S.; Wang, S.; Li, Y.; Xu, H.; Wang, D. Self-assembled composite nanoparticles based on zein as delivery vehicles of curcumin: Role of chondroitin sulfate. *Food Funct.* **2020**, *11*, 5377–5388. [[CrossRef](#)] [[PubMed](#)]
43. Berdiaki, A.; Perisynaki, E.; Stratidakis, A.; Kulikov, P.P.; Kuskov, A.N.; Stivaktakis, P.; Henrich-Noak, P.; Luss, A.L.; Shtilman, M.I.; Tzanakakis, G.N.; et al. Assessment of Amphiphilic Poly-N-vinylpyrrolidone Nanoparticles' Biocompatibility with Endothelial Cells in Vitro and Delivery of an Anti-Inflammatory Drug. *Mol. Pharm.* **2020**, *17*, 4212–4225. [[CrossRef](#)] [[PubMed](#)]
44. Estifeeva, T.M.; Barmin, R.A.; Rudakovskaya, P.G.; Nechaeva, A.M.; Luss, A.L.; Mezhev, Y.O.; Chernyshev, V.S.; Krivoborodov, E.G.; Klimenko, O.A.; Sindeeva, O.A.; et al. Hybrid (Bovine Serum Albumin)/Poly(N-vinyl-2-pyrrolidone-co-acrylic acid)-Shelled Microbubbles as Advanced Ultrasound Contrast Agents. *ACS Appl. Bio Mater.* **2022**, *5*, 3338–3348. [[CrossRef](#)] [[PubMed](#)]
45. Schneider, C.A.; Rasband, W.S.; Eliceiri, K.W. NIH Image to ImageJ: 25 years of image analysis. *Nat. Methods* **2012**, *9*, 671–675. [[CrossRef](#)] [[PubMed](#)]
46. Yaminsky, I.; Akhmetova, A.; Meshkov, G. Femtoscan online software and visualization of nano-objects in high-resolution microscopy. *Nanoindustry* **2018**, *11*, 44–48. [[CrossRef](#)]
47. Ranjan, A.P.; Mukerjee, A.; Helson, L.; Vishwanatha, J.K. Scale up, optimization and stability analysis of Curcumin C3 complex-loaded nanoparticles for cancer therapy. *J. Nanobiotechnol.* **2012**, *10*, 38. [[CrossRef](#)] [[PubMed](#)]
48. Hasan, M.; Latifi, S.; Kahn, C.; Tamayol, A.; Habibey, R.; Passeri, E.; Linder, M.; Arab-Tehrany, E. The Positive Role of Curcumin-Loaded Salmon Nanoliposomes on the Culture of Primary Cortical Neurons. *Mar. Drugs* **2018**, *16*, 218. [[CrossRef](#)] [[PubMed](#)]
49. Hasan, M.; Elkhoury, K.; Kahn, C.; Arab-Tehrany, E.; Linder, M. Preparation, Characterization, and Release Kinetics of Chitosan-Coated Nanoliposomes Encapsulating Curcumin in Simulated Environments. *Molecules* **2019**, *24*, 2023. [[CrossRef](#)]
50. von Hellfeld, R.; Brotzmann, K.; Baumann, L.; Strecker, R.; Braunbeck, T. Adverse effects in the fish embryo acute toxicity (FET) test: A catalogue of unspecific morphological changes versus more specific effects in zebrafish (*Danio rerio*) embryos. *Environ. Sci. Eur.* **2020**, *32*, 122. [[CrossRef](#)]
51. Bagrov, D.V.; Adlerberg, V.V.; Skryabin, G.O.; Nikishin, I.I.; Galetsky, S.A.; Tchevkina, E.M.; Kirpichnikov, M.P.; Shaitan, K.V. AFM-TEM correlation microscopy and its application to lipid nanoparticles. *Microsc. Res. Tech.* **2023**, *86*, 781–790. [[CrossRef](#)]
52. Ito, T.; Sun, L.; Bevan, M.A.; Crooks, R.M. Comparison of nanoparticle size and electrophoretic mobility measurements using a carbon-nanotube-based coulter counter, dynamic light scattering, transmission electron microscopy, and phase analysis light scattering. *Langmuir* **2004**, *20*, 6940–6945. [[CrossRef](#)]
53. Liu, Z.; Lansley, A.B.; Duong, T.N.; John, D.S.; Pannala, A.S. Increasing Cellular Uptake and Permeation of Curcumin Using a Novel Polymer-Surfactant Formulation. *Biomolecules* **2022**, *12*, 1739. [[CrossRef](#)] [[PubMed](#)]
54. Huang, L.; Cai, M.; Xie, X.; Chen, Y.; Luo, X. Uptake enhancement of curcumin encapsulated into phosphatidylcholine-shielding micelles by cancer cells. *J. Biomater. Sci. Polym. Ed.* **2014**, *25*, 1407–1424. [[CrossRef](#)] [[PubMed](#)]
55. Loufakis, D.N.; Cao, Z.; Ma, S.; Mittelman, D.; Lu, C. Focusing of mammalian cells under an ultrahigh pH gradient created by unidirectional electropulsation in a confined microchamber. *Chem. Sci.* **2014**, *5*, 3331. [[CrossRef](#)] [[PubMed](#)]
56. Metwally, S.; Stachewicz, U. Surface potential and charges impact on cell responses on biomaterials interfaces for medical applications. *Mater. Sci. Eng. C Mater. Biol. Appl.* **2019**, *104*, 109883. [[CrossRef](#)] [[PubMed](#)]
57. Kuskov, A.N.; Kulikov, P.P.; Goryachaya, A.V.; Tzatzarakis, M.N.; Tsatsakis, A.M.; Velonia, K.; Shtilman, M.I. Self-assembled amphiphilic poly-N-vinylpyrrolidone nanoparticles as carriers for hydrophobic drugs: Stability aspects. *J. Appl. Polym. Sci.* **2017**, *135*, 45637. [[CrossRef](#)]
58. Ebenstein, Y.; Nahum, E.; Banin, U. Tapping Mode Atomic Force Microscopy for Nanoparticle Sizing: Tip–Sample Interaction Effects. *Nano Lett.* **2002**, *2*, 945–950. [[CrossRef](#)]
59. Moiseenko, A.V.; Bagrov, D.V.; Vorovitch, M.F.; Uvarova, V.I.; Veselov, M.M.; Kashchenko, A.V.; Ivanova, A.L.; Osolodkin, D.I.; Egorov, A.M.; Ishmukhametov, A.A.; et al. Size Distribution of Inactivated Tick-Borne Encephalitis Virus Particles Revealed by a Comprehensive Physicochemical Approach. *Biomedicines* **2022**, *10*, 2478. [[CrossRef](#)]
60. Bagrov, D.V.; Glukhov, G.S.; Moiseenko, A.V.; Karlova, M.G.; Litvinov, D.S.; Zaitsev, P.A.; Kozlovskaya, L.I.; Shishova, A.A.; Kovpak, A.A.; Ivin, Y.Y.; et al. Structural characterization of β -propiolactone inactivated severe acute respiratory syndrome coronavirus 2 (SARS-CoV-2) particles. *Microsc. Res. Tech.* **2022**, *85*, 562–569. [[CrossRef](#)]
61. Klinov, D.V.; Dubrovin, E.V.; Yaminsky, I.V. Scanning Probe Microscopy of DNA on Mica and Graphite. *AIP Conf. Proc.* **2003**, *696*, 452–456.

62. Labanca, F.; Ullah, H.; Khan, H.; Milella, L.; Xiao, J.; Dajic-Stevanovic, Z.; Jeandet, P. Therapeutic and Mechanistic Effects of Curcumin in Huntington's Disease. *Curr. Neuropharmacol.* **2021**, *19*, 1007–1018. [[CrossRef](#)] [[PubMed](#)]
63. Persano, F.; Gigli, G.; Leporatti, S. Natural Compounds as Promising Adjuvant Agents in The Treatment of Gliomas. *Int. J. Mol. Sci.* **2022**, *23*, 3360. [[CrossRef](#)] [[PubMed](#)]
64. Wei, H.; Jiang, D.; Yu, B.; Ni, D.; Li, M.; Long, Y.; Ellison, P.A.; Siamof, C.M.; Cheng, L.; Barnhart, T.E.; et al. Nanostructured polyvinylpyrrolidone-curcumin conjugates allowed for kidney-targeted treatment of cisplatin induced acute kidney injury. *Bioact. Mater.* **2023**, *19*, 282–291. [[CrossRef](#)]
65. Tsatsakis, A.; Stratidakis, A.K.; Goryachaya, A.V.; Tzatzarakis, M.N.; Stivaktakis, P.D.; Docea, A.O.; Berdiaki, A.; Nikitovich, D.; Velonia, K.; Shtilman, M.I.; et al. In vitro blood compatibility and in vitro cytotoxicity of amphiphilic poly-N-vinylpyrrolidone nanoparticles. *Food Chem. Toxicol.* **2019**, *127*, 42–52. [[CrossRef](#)] [[PubMed](#)]
66. Kuskov, A.N.; Kulikov, P.P.; Shtilman, M.I.; Rakitskii, V.N.; Tsatsakis, A.M. Amphiphilic poly-N-vinylpyrrolidone nanoparticles: Cytotoxicity and acute toxicity study. *Food Chem. Toxicol.* **2016**, *96*, 273–279. [[CrossRef](#)] [[PubMed](#)]
67. Gholami, L.; Momtazi-Borojeni, A.A.; Malaekheh-Nikouei, B.; Nikfar, B.; Amanolahi, F.; Mohammadi, A.; Oskuee, R.K. Selective Cellular Uptake and Cytotoxicity of Curcumin-encapsulated SPC and HSPC Liposome Nanoparticles on Human Bladder Cancer Cells. *Curr. Pharm. Des.* **2023**, *29*, 1046–1058. [[CrossRef](#)]
68. Bolger, G.T.; Licollari, A.; Bagshaw, R.; Tan, A.; Greil, R.; Vcelar, B.; Majeed, M.; Sordillo, P. Intense Uptake of Liposomal Curcumin by Multiple Myeloma Cell Lines: Comparison to Normal Lymphocytes, Red Blood Cells and Chronic Lymphocytic Leukemia Cells. *Anticancer Res.* **2019**, *39*, 1161–1168. [[CrossRef](#)]
69. Apiratikul, N.; Penglong, T.; Suksen, K.; Svasti, S.; Chairoungdua, A.; Yingyongnarongkul, B. In vitro Delivery of Curcumin with Cholesterol-Based Cationic Liposomes. *Russ. J. Bioorg. Chem.* **2013**, *39*, 444–450. [[CrossRef](#)]
70. Bi, C.; Miao, X.Q.; Chow, S.F.; Wu, W.J.; Yan, R.; Liao, Y.H.; Chow, A.H.-L.; Zheng, Y. Particle size effect of curcumin nanosuspensions on cytotoxicity, cellular internalization, in vivo pharmacokinetics and biodistribution. *Nanomedicine* **2017**, *13*, 943–953. [[CrossRef](#)]
71. Hesari, A.; Rezaei, M.; Rezaei, M.; Dashtiahangar, M.; Fathi, M.; Rad, J.G.; Momeni, F.; Avan, A.; Ghasemi, F. Effect of curcumin on glioblastoma cells. *J. Cell Physiol.* **2019**, *234*, 10281–10288. [[CrossRef](#)]
72. Weissenberger, J.; Priester, M.; Bernreuther, C.; Rakel, S.; Glatzel, M.; Seifert, V.; Kögel, D. Dietary curcumin attenuates glioma growth in a syngeneic mouse model by inhibition of the JAK1,2/STAT3 signaling pathway. *Clin. Cancer Res.* **2010**, *16*, 5781–5795. [[CrossRef](#)] [[PubMed](#)]
73. Shahcheraghi, S.H.; Zangui, M.; Lotfi, M.; Ghayour-Mobarhan, M.; Ghorbani, A.; Jaliani, H.Z.; Sadeghnia, H.R.; Sahebkar, A. Therapeutic Potential of Curcumin in the Treatment of Glioblastoma Multiforme. *Curr. Pharm. Des.* **2019**, *25*, 333–342. [[CrossRef](#)] [[PubMed](#)]
74. Ryskalin, L.; Biagioni, F.; Busceti, C.L.; Lazzeri, G.; Frati, A.; Fornai, F. The Multi-Faceted Effect of Curcumin in Glioblastoma from Rescuing Cell Clearance to Autophagy-Independent Effects. *Molecules* **2020**, *25*, 4839. [[CrossRef](#)] [[PubMed](#)]
75. Zoi, V.; Galani, V.; Vartholomatos, E.; Zacharopoulou, N.; Tsoumeleka, E.; Gkizas, G.; Bozios, G.; Tsekeris, P.; Chousidis, I.; Leonardos, I.; et al. Curcumin and Radiotherapy Exert Synergistic Anti-Glioma Effect In Vitro. *Biomedicines* **2021**, *9*, 1562. [[CrossRef](#)]

Disclaimer/Publisher's Note: The statements, opinions and data contained in all publications are solely those of the individual author(s) and contributor(s) and not of MDPI and/or the editor(s). MDPI and/or the editor(s) disclaim responsibility for any injury to people or property resulting from any ideas, methods, instructions or products referred to in the content.